Effect of Heat Loss on Laminar Flamelet Species Concentration

Marco Boccanera, Diego Lentini

Dipartimento di Ingegneria Meccanica e Aerospaziale, Sapienza Università di Roma, Via Eudossiana 18, 00184 Rome, Italy

The effects of heat loss on the structure of laminar flamelets, which are the constitutive elements of turbulent flames under the most common operating conditions, are investigated for typical aeronautical gas-turbine operating conditions at take-off. The magnitude of heat loss is quantified via the "enthalpy defect" measured with respect to an adiabatic flame. A procedure to generate laminar flamelets with an assigned enthalpy defect at the boundaries is devised and applied to nonpremixed propane/air flames, as propane reproduces the essential features of higher hydrocarbon combustion. It is found, contrary to commonly held beliefs, that the enthalpy defect has a significant effect on the concentration not only of minor species, but also of main reaction products. Such effects are found in general to be more pronounced for fuel-rich conditions. An impact is anticipated on the formation rate of nitric oxides. The effects of scalar dissipation rate are also discussed.

Keywords: Turbulent Combustion, Heat Transfer, Laminar Flamelets, Hydrocarbon Combustion, Aeroengines, Gas Turbines

Introduction

Models for turbulent combustion in industrial applications lean heavily on the "laminar flamelet" approach [1-5] which, under suitable assumptions which are found to hold in most cases, reduces the value of any state quantity φ (e.g., density, temperature, concentrations, etc.) in a laminar flame to a function of a single quantity, the conserved scalar (or mixture fraction) Z, with the meaning both of a suitably scaled elemental mass fraction (or a linear combination of the mass fractions of the different elements) and, under the assumption of equal diffusivities, of a scaled enthalpy:

$$\varphi = \varphi(Z) \qquad (1)$$

In turbulent flows, the *mean* value of the state quantity under consideration can be recovered by introducing an appropriately defined probability density function (pdf) of the conserved scalar, and then convoluting Eq. (1) with this pdf. Higher scalar moments, such as variances, can also be obtained in a similar way.

The model can be extended to account for finite-rate chemistry (albeit limited to relatively small departures from equilibrium) by introducing a second fundamental state quantity, the scalar dissipation rate conditioned at the flame front (e.g., at stoichiometric, or at the location of peak temperature, or peak heat release), denoted as χ_c. In this approach, termed "stretched laminar flamelet" [6-9], any state quantity can accordingly be expressed as a function of these two quantities:

$$\varphi = \varphi(Z, \chi_c) \qquad (2)$$

and evaluation of mean values in turbulent flows requires the introduction of a joint pdf of Z and χ_c, which is still manageable. The functions (2) are evaluated by dedicated codes handling complex chemical kinetics and detailed transport for counterflowing jets of fuel and oxidizer, which allow (once an appropriate definition of the conserved scalar is put forth) to recover all state quantities as a function of Z. The conditioned scalar dissipation rate χ_c acts as a parameter (specified indirectly by assigning the velocity of the two counterflowing jets), which must be varied from near-zero (equilibrium) to the quenching limit χ_q. For $\chi_c > \chi_q$, the flamelet is extinguished, and state quantities do not depend any longer on χ_c.

In high-temperature combustion, heat loss effects (by radiation in particular) have a direct bearing on state relationships; in such circumstances, a third fundamental state quantity is required to define state functions in laminar flamelets (incidentally, Z no longer represents enthalpy in this case). The radiant fraction (fraction of combustion-generated heat lost by radiation) is sometimes used [10]; laminar flamelet profiles for the non-adiabatic case at hand are then derived by *ad hoc* adjustments of the corresponding adiabatic profiles (e.g., see [11]). A more rigorous approach [12] involves introducing the enthalpy defect (difference between the enthalpy of two flamelets, one adiabatic, the other undergoing heat transfer, for the same value of Z). Non-adiabatic flamelets can be calculated by enforcing appropriate boundary conditions (see next Section), and lead to the form

$$\varphi = \varphi (Z, \chi_c, \zeta) \qquad (3)$$

which requires a three-variable pdf for evaluating mean values in turbulent flames. Adopting the three-variable approach accordingly necessitates a very extensive flamelet "library", with both χ_c and ζ as a parameter. We refer to the whole of the flamelets with a given enthalpy defect as to a "shelf", and in particular, for $\zeta = 0$, as to the "adiabatic shelf". In order to get an accurate solution, each shelf may require from 10 to 20 flamelets (with different values of χ_c), and in highly radiating flames, as many as 15 shelves are used [13, 14]. This means that, on the whole, computation of quite a few hundred flamelets is required. Although the computation is performed off-line, this involves a substantial amount of computational work.

This is most often avoided in models of current usage by invoking independence of species concentration on the enthalpy defect (or, somewhat equivalently, on the radiant fraction), and consequently assuming that heat transfer affects only temperature (and density). This assumption is generally thought to be well verified for major species, but in a study [15] concerning a syngas/air flame (syngas is a mixture of 40% CO, 30% H_2, 30% N_2 in volume), the authors find that concentration of some minor species is significantly affected by the enthalpy defect (despite the fact that relatively limited enthalpy defects, down to -80 kJ/kg only, are considered there).

Moving on these grounds, a more ambitious investigation is carried out in the present paper, aimed at generating a flamelet library to be used to model gas-turbine combustion at typical take-off conditions. In this case, air is preheated to a high temperature in the compressor, while the fuel is liquid kerosene. However, owing to the high air temperature, fuel burns effectively very much like a vapour [16] (at least at full power operation), then phase transition effects can be neglected. Further, higher hydrocarbon chemistry is extremely complex, and a universally accepted reaction mechanism does not exist. Nonetheless, it is well known that propane closely reproduces the main features of higher hydrocarbon combustion, and kerosene in particular [17]. Accordingly, fuel is modelled as propane in this study, and typical gas-turbine inlet conditions at take-off (T_{air} = 852 K, p = 2.985 MPa) are considered. The main focus of the present paper is on results concerning flamelets subjected to low strain (corresponding to a scalar dissipation rate $\chi_c \sim 0.4\ s^{-1}$), but some results are also reported relative to a more extensive investigation concerning flamelets with strain rates up to extinction, though limited to the adiabatic shelf for the sake of conciseness.

In the next Section, the computational procedure is concisely outlined, whereas results are reported in the subsequent Section.

Computational Procedure

Flamelets are computed by means of the OPPDIF code [18], with detailed transport properties and thermal diffusion included. The reaction mechanism is taken after Peters and Rogg [19], including 34 species (up to C_3-) and 87 reversible reactions.

In order to account for heat transfer, the flamelet library is organized in "shelves". The "adiabatic" shelf is computed by enforcing temperature boundary conditions corresponding to the nominal temperatures of oxidizer and fuel (T_{air} = 852 K, T_{fuel} = 300 K), at the respective sides. In order to account for heat losses, nonadiabatic shelves are introduced, with lower boundary temperatures with respect to the adiabatic reference shelf. If the assumption of unity Lewis numbers for all species is retained, it is possible to compute a shelf with a uniform enthalpy defect by merely assigning appropriate boundary temperatures. However, when differential diffusion is introduced, assigning appropriate temperatures at the extremes does no longer allow a uniform enthalpy defect across the flamelet. In the following we therefore adopt the enthalpy defect at the boundaries (oxidizer and fuel side), denoted as ζ_b, as the parameter to quantify the effect of heat losses, with the understanding however that the enthalpy defect ζ across the flamelet will not be uniform at the value ζ_b (see also Fig. 1 below).

Assume that shelf denoted by index m (i.e., with a specified value of ζ) has already been computed, and that another shelf $m+1$ is going to be computed, featuring an additional enthalpy defect $\Delta\zeta$ (negative) with respect to the former. The boundary conditions (temperature and species concentration) at the oxidizer and fuel sides must be derived accordingly. An immediate way to enforce the requested enthalpy defect at the extremes is to lower the corresponding temperatures, so that the oxidizer and fuel

enthalpies exhibit the requested defect $\zeta+\Delta\zeta$ with respect to the adiabatic shelf. This procedure however is limited to small enthalpy defects, because as the temperature is reduced below ambient the gases soon condense, or anyway lose their perfect-gas behaviour. An alternative, more general procedure is therefore required.

To this end, we observe that, for a given value of the conserved scalar Z, the temperature drops rapidly as the enthalpy is reduced, while the species concentrations experience only relatively minor changes close to the oxidizer and fuel sides (while significant differences may arise closer to stoichiometric). With this in mind, the following procedure is suggested. The mixture enthalpy is related to temperature and composition as

$$h = \Sigma_i Y_i h_i (T) \quad (4)$$

If the composition of the mixture of N species is known, and the enthalpy is assigned, this can be easily inverted to recover the corresponding temperature

$$T = T (h, Y_1, Y_2, \ldots, Y_N) \quad (5)$$

Points of shelf m close to the boundaries can be processed after Eq. (5), with enthalpy assigned as the relevant enthalpy of shelf m, diminished by $\Delta\zeta$, and with fixed composition. The first point, moving away from the boundary, for which the resulting temperature turns out to be equal or greater than a prescribed temperature T^*, e.g., the ambient temperature (incidentally, different T^*'s might be assigned at the two sides, if required), is chosen to enforce the boundary condition for shelf $m+1$.

When detailed transport properties are introduced, further problems arise in the definition of the flamelet library. While dedicated computational codes compute flamelets in physical space, these must be converted in conserved scalar space in order to be used by turbulent combustion models. Unfortunately, the definition of conserved scalar is ambiguous in the presence of differential diffusion. The problem is tackled in the literature by introducing heuristic definitions of the conserved scalar, aimed at obtaining a monotonic trend of the conserved scalar Z vs. the physical coordinate x. In the present study, Z is defined in terms of a scaled mass fraction of element nitrogen, Z_N:

$$Z = (Z_N - Z_{N,air}) / (Z_{N,\,fuel} - Z_{N,\,air}) \quad (6)$$

where $Z_{N,\,air}$ and $Z_{N,\,fuel}$ denote the nitrogen elemental mass fractions in the oxidizer and fuel stream, respectively (the latter being zero in the present case). This is found to produce the desired monotonic behavior.

Results

The procedure described above to assign the enthalpy defect for the shelf under consideration ensures that the flamelet features the required enthalpy defect at the boundaries, i.e., at the oxidizer and fuel sides. However, due to the effect of differential diffusion, the enthalpy defect will not be uniform across the flamelet thickness, as indicated in Fig. 1. It is in principle possible to compute the properties of a 'pseudo-flamelet' with uniform enthalpy defect by interpolating between adjacent shelves; this would make the application to turbulent combustion models straightforward. The discretization error inherent in the interpolation procedure can be reduced to an arbitrarily small proportion by adopting a suitably small $\Delta\zeta$ between adiacent shelves. The interpolation procedure is important in applications to turbulent flames, but represents anyway a sort of higher-order correction to the flamelet profiles. Accordingly, it is not considered in the following comments, mainly focused at emphasizing that *there is* an effect of the enthalpy level on species concentrations. The range of enthalpy defects at the boundaries, ζ_b, considered in this test case is 0 (adiabatic), −50 kJ/kg, −100 kJ/kg, −150 kJ/kg and –200 kJ/kg.

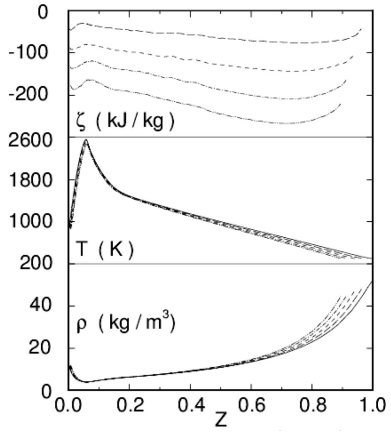

Fig. 1 Enthalpy defect, temperature, density: solid line ζ_b=0, long-dashed line ζ_b= −50 kJ/kg, short-dashed line ζ_b= −100 kJ/kg, dash-dotted line ζ_b= −150 kJ/kg, dash-double dotted line ζ_b= −200 kJ/kg.

Incidentally, even larger enthalpy defects may take place in furnaces, thereby further stressing the need to correctly account for the effects under consideration.

In analyzing the results below, it must be borne in mind that stoichiometric conditions for propane/air combustion corresponds to the value Z_{st} = 0.07.

Figure 1 also shows the effect of the enthalpy defect on temperature profiles, as well as the ensuing effect on density (although the latter is also affected by the mixture molecular weight, varying with composition). Temperature is of course reduced when increasingly negative enthalpy defects are considered, with the effect being more apparent at the fuel boundary. For instance, the peak temperature of the adiabatic flamelet is 2562 K, which is reduced to 2464 for ζ_b = −200 kJ/kg. It is also noted that the range of Z spanned by the different curves is reduced

with increasingly negative ζ_b's, as a result of the procedure described in the previous Section to avoid unrealistically low temperatures at the boundaries. The high numerical values for the density are due to the high pressure conditions under consideration.

Figure 2 reports the concentration of major chemical species, in terms of mass fractions. In particular, the enthalpy defect is seen to have a major impact on molecular hydrogen H_2. While its peak concentration is nearly unaffected, flames with highly negative enthalpy defects feature a major increase of H_2 concentration near the fuel side, with the appearance of a secondary peak which eventually becomes even higher than the one of the adiabatic flamelet.

Molecular oxygen O_2 concentration is seen to increase with increasingly negative enthalpy defects, indicating that combustion is less complete. For instance, if we focus on O_2 concentration at Z=0.02, it is found that for ζ_b = −200 kJ/kg this is increased by 13% relative to the adiabatic flamelet. No O_2 is found beyond stoichiometric (but this is no longer the case for higher χ_cs, see Fig. 4 below).

Concentration of propane C_3H_8 is somewhat affected by the enthalpy defect, even though the effect is not apparent due to the fact that the ordinate scale spans the full range zero to unity. Notice that no overlap is seen between O_2 and C_3H_8 at the low value of χ_c under consideration; the picture is different for higher χ_cs, i.e., increasing finite-rate chemistry effects, in which case some overlap is apparent, similar to what is shown in Fig. 4 below for molecular oxgen.

An important effect is observed on water gas H_2O, which is the major reaction product (together with CO_2, and eventually CO). Peak concentration is seen to increase about 15% with respect to adiabatic for ζ_b = −200 kJ/kg, thus underlining the need to accurately account for enthalpy defect effects in combustion models.

Another important species featuring a marked effect of the enthalpy defect is carbon monoxide CO, with the peak value decreasing about 25% (with respect to adiabatic) in the range mentioned above. It is anyway seen that CO concentration is important only for mixtures operating near stoichiometric and fuel-rich, which is not the case for gas turbines. It is anyway safe to say that CO predictions are subjected to considerable uncertainty.

The resulting effect on CO_2 turns out instead to be much less significant, in the range of about 2% (with respect to adiabatic).

Methane CH_4 represents (together with other species, see below) unburnt hydrocarbons; its concentration is seen to be somewhat affected by the enthalpy defect for Z>0.17.

Acetylene C_2H_2 is important both as an unburnt hydrocarbon, and a precursor of soot formation. It appears in significant concentrations in fuel-rich combustion, and it is seen to show some dependence on the enthalpy defect for Z>0.13.

Another unburnt hydrocarbon is ethylene C_2H_4, which is seen to be relatively sensitive to the enthalpy defect for Z>0.18.

Concentrations of some minor chemical species are reported in Fig. 3. As they occur in appreciable proportions only near stoichiometric, the range of the conserved scalar reported in the Figures is in this case restricted to [0, 0.2]. The enthalpy defect is seen to produce an appreciable effect on atomic hydrogen H concentration, with a peak value reduced by 30% on a relative basis when passing from the adiabatic flamelet to the ζ_b = −200 kJ/kg one.

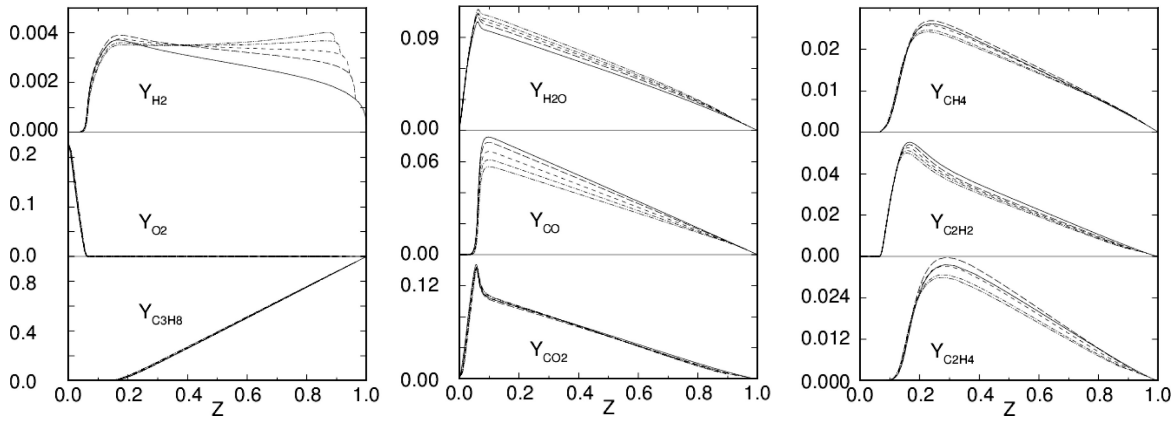

Fig. 2 Concentration of major species: solid line ζ_b=0, long-dashed line ζ_b= -50 kJ/kg, short-dashed line ζ_b= −100 kJ/kg, dash-dotted line ζ_b= −150kJ/kg, dash-double dotted line ζ_b= −200 kJ/kg.

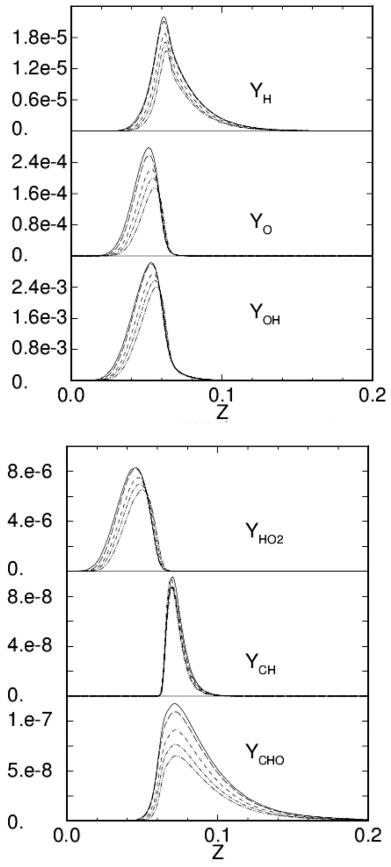

Fig. 3 Concentration of minor species: solid line ζ_b=0, long-dashed line ζ_b= -50 kJ/kg, short-dashed line ζ_b= −100 kJ/kg, dash-dotted line ζ_b= -150kJ/kg, dash-double dotted line ζ_b= −200 kJ/kg.

A particularly important effect is noted for atomic oxygen O, with peak concentration decreasing by over 35% in the same range as above. This species is relevant to nitric oxide emissions, as the production term due to the thermal mechanism can be expressed as

$$w_{NO,th} = 2M_{NO}B_1T^{\alpha_1}\exp\left(-\frac{E_1}{R^0T}\right)\cdot\rho^2\frac{Y_o}{M_o}\frac{Y_{N2}}{M_{N2}} \quad (7)$$

where the M_is indicate molar masses, and rate constants refer to the rate-limiting reaction

$$N_2 + O \rightarrow NO + N \quad (8)$$

The effect of reduced oxygen concentration with increasingly negative ζ adds up to the accompanying temperature decrease. It is therefore expected that taking into account the effect of enthalpy defect can lead to refined predictions of nitrogen oxide emissions from flames and combustors.

Hydroxil OH, which affects soot oxidation, is another rate-limited species, and is seen to be significantly affected by the enthalpy defect (peak concentration reduced by up to 20% in the range quoted). Anyway, it is also very sensitive to χc.

The reaction intermediate hydrogen peroxide H_2O_2 also shows a significant effect of ζ (peak reduced by over 20%).

Methylidyne CH is closely associated with formation of prompt NO; the enthalpy defect appears to bring about relatively minor effects on its concentrations. At any rate, level are so small that significant formation of prompt NO seems unlikely (though this might be an effect of the approximation involved in identifying fuel as propane).

Formyl CHO is seen to occur in trace concentration only. Anyway, it is often used as a reaction zone marker in hydrocarbon combustion; its concentration is observed to be very sensitive to enthalpy defect, as the peak is reduced by over 40% when passing from adiabatic to ζ_b = −200 kJ/kg.

Lastly, some effects of the impact of finite-rate chemistry, as identified by the conditioned scalar dissipation rate χ_c, are reported in Fig. 4 for the adiabatic shelf only. As many as 17 flamelets, for stretch conditions ranging from near-equilibrium to near-extinction (which is found to occur beyond χ_c = 327 s^{-1}) have been generated, though only 5, plus the inert mixing state, are shown in the Figure in order to avoid clutter. It is seen that while in near-equilibrium conditions the mass fraction of molecular oxygen is basically zero beyond stoichiometric, for increasing χ_cs some oxygen can survive on the rich side of the flame due to insufficient residence time for complete combustion. Further, acetylene concentration is shown to be quite sensitive to stretch conditions, with an attendant significant effect on soot formation. Similar significant effects are found for the concentration of atomic oxygen, appearing in Eq. (7) for the nitric oxide formation rate, and of hydroxyl, an important soot-oxidizing agent.

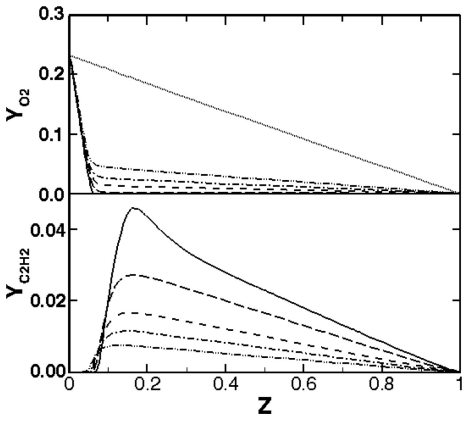

Fig. 4 Concentration of molecular oxygen and acetylene: solid line χ_c= 0.4 s^{-1}, long-dashed line χ_c = 82 s^{-1}, short-dashed line χ_c = 278 s^{-1}, dash-dotted line χ_c = 309 s^{-1}, dash-double dotted line χ_c = 327 s^{-1} , dotted line inert state.

Conclusions

Present results emphasize the need to correctly account for the effect of heat loss on the concentration of chemical species in laminar flamelets, which in turn are the thermochemical database passed as an input to turbulent combustion models. Effects are seen to be quite remarkable not only for minor species, but also for some major reaction products such as H_2O and CO. Effects are in general more pronounced at the fuel side, though significant effects are also seen for O_2, which is only present at the lean side (at least for the low value of χ_c considered in this study). Further, it is as well to remark that the range of enthalpy defects considered in this study is quite limited with respect to the one which can actually take place in furnaces, where heat transfer to the wall is the goal.

Future work will involve exploration of the feasibility and possible advantage of the approach of the 'pseudo-flamelets' with uniform enthalpy defect ζ, to be generated by interpolation, and the evaluation of the effect of heat losses on rate-limited species, such as nitric oxide.

References

[1] Hawthorne, R.W., Weddell, D.S. and Hottel, H.C., Mixing and combustion in turbulent gas jets, 3rd Symp. Comb., Flame Expl. Phen., Williams and Wilkins, Baltimore, 1949, pp. 266–288.

[2] Bilger, R. W., Turbulent flows with nonpremixed reactants, in Turbulent Reacting Flows (Libby, P.A. and Williams, F.A., Eds.), Springer-Verlag, Berlin, 1980, pp. 65–113.

[3] N. Peters, Turbulent Combustion, Cambridge Univ. Press, 2004.

[4] N. Peters, Combustion Theory, CEFRC Summer School, Princeton, 2010.

[5] Cuenot, B., The flamelet model for non-premixed combustion, in Turbulent Combustion Modeling (Echekki, T. and Mastorakas, E., Eds.), Springer-Verlag, Berlin, 2011, pp. 43–63.

[6] Liew, S.K., Bray, K.N.C. and Moss, J.B., A stretched laminar flamelet model of turbulent nonpremixed combustion, Combust. Flame, Vol. 56, pp. 199–213, 1984.

[7] Peters, N., Laminar diffusion flamelet models in non-premixed turbulent combustion, Prog. Energy Combust. Sci., Vol. 10, pp. 319–339, 1984.

[8] Lentini, D., Assessment of the stretched laminar flamelet approach for nonpremixed turbulent combustion, Combust. Sci. and Tech., Vol. 100, pp. 95–122, 1994.

[9] Lentini, D. and Puri, I.K., Stretched laminar flamelet modeling of turbulent chloromethane-air nonpremixed jet flames, Combust. Flame, Vol. 103, pp. 328–338, 1995.

[10] Modest, M.F. and Haworth, D.C., Radiative Heat Transfer in Turbulent Combustion Systems, Springer, Berlin, Heidelberg, Germany, 2016.

[11] Fairweather, M., Jones, W.P., Lindstedt, R.P. and Marquis, A.J., Predictions of a turbulent reacting jet in a cross-flow, Combust. Flame, Vol. 84, pp. 361–375, 1991.

[12] Bray, K.N.C. and Peters, N., Laminar flamelets in turbulent flames, in Turbulent Reacting Flows (Libby, P.A. and Williams, F.A., Eds.), Academic Press, London, 1994, pp. 63–113.

[13] Marracino, B. and Lentini, D., Radiation modelling in non-luminous nonpremixed turbulent flames, Combust. Sci. and Tech., Vol. 128, pp. 23–48, 1997.

[14] Giordano, P. and Lentini, D., Combustion-radiation-turbulence interaction modeling in absorbing/emitting nonpremixed flames, Combust. Sci. and Tech, Vol. 172, pp. 1–22, 2001.

[15] Boccanera, M. and Lentini, D., Extensive stretched laminar flamelet library with enthalpy defect for syngas/air combustion, AIAA paper 2001-3421, Salt Lake City, 2001.

[16] Jones, W.P. and Whitelaw, J.H., Modelling and measurements in turbulent combustion, 20th Symp. (Int.) on Combust., The Combustion Institute, Pittsburgh, 1984, pp. 233–249.

[17] Turns, S.R. and Lovett, J.A., Measurements of oxides of nitrogen emissions from turbulent propane jet diffusion flames, Combust. Sci. and Tech., Vol. 66, pp. 233–249, 1989.

[18] Lutz, A.E., Kee, R.J., Grcar, J.F. and Rupley, F.M., OPPDIF: a Fortran program for computing opposed flow diffusion flames, Rept. SAND 96–8243, 1997.

[19] Peters, N. and Rogg, B., Reduced Kinetic Reaction Mechanisms for Application in Combustion Systems, Springer-Verlag, Berlin, 1993.